Supporting Information

Pyridylpyrazole N^N Ligands Combined with Sulfonyl-Functionalized Cyclometalating Ligands for Blue-Emitting Iridium(III) Complexes and Solution-Processable PhOLEDs

Helen Benjamin,[†] Mark A. Fox,[†] Andrei S. Batsanov,[†] Hameed A. Al-Attar,[‡] Chensen Li, [§] Zhongjie Ren,[§] Andrew P. Monkman,[‡] and Martin R. Bryce*,[†]

[†]*Department of Chemistry, Durham University, Durham DH1 3LE, U.K.* *m.r.bryce@durham.ac.uk*

[‡] *Department of Physics, Durham University, Durham DH1 3LE, U.K.*

[§] *State Key Laboratory of Chemical Resource Engineering, Beijing University of Chemical Technology, Beijing 100029, China*

Contents

Copies of NMR spectra

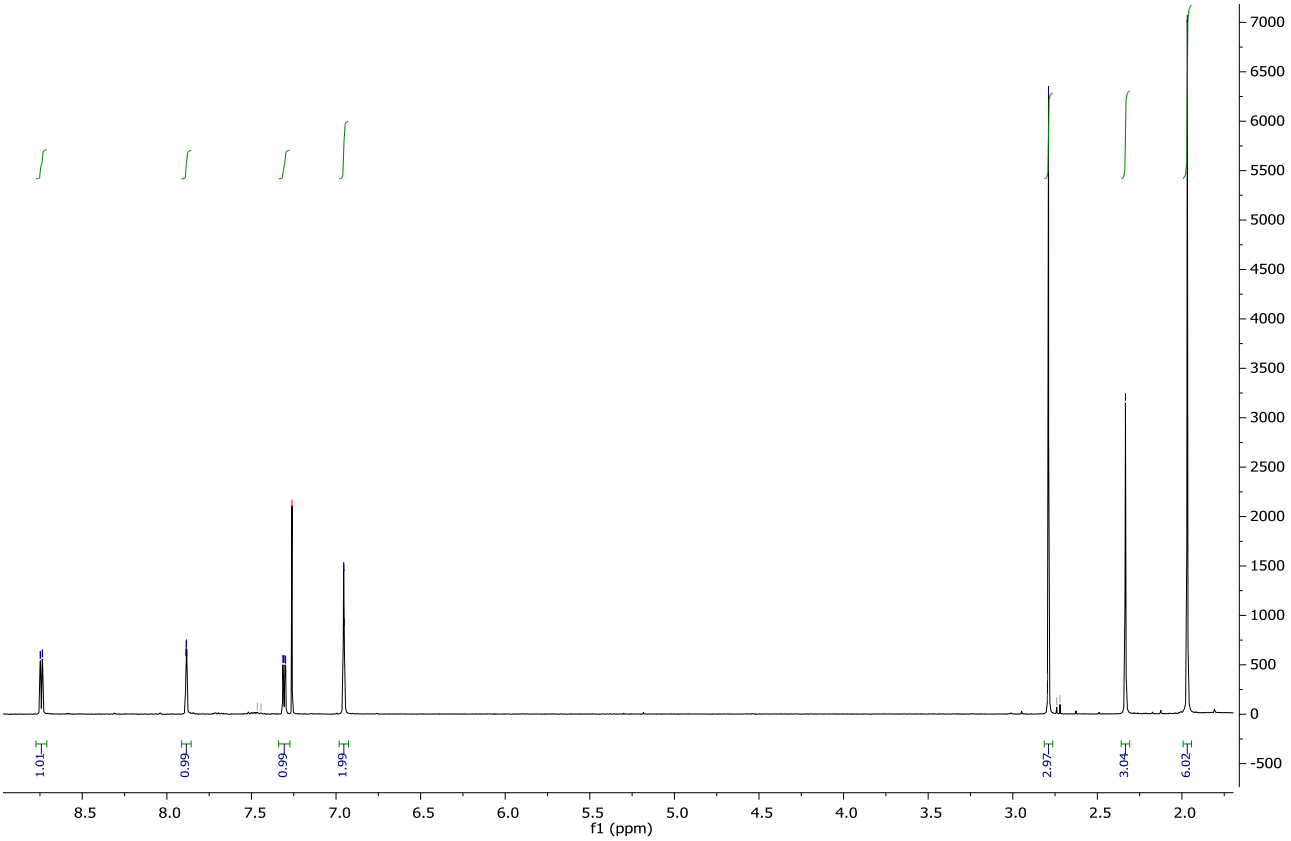

Figure S1. ^{1}H NMR spectrum of **7** in $CDCl_3$.

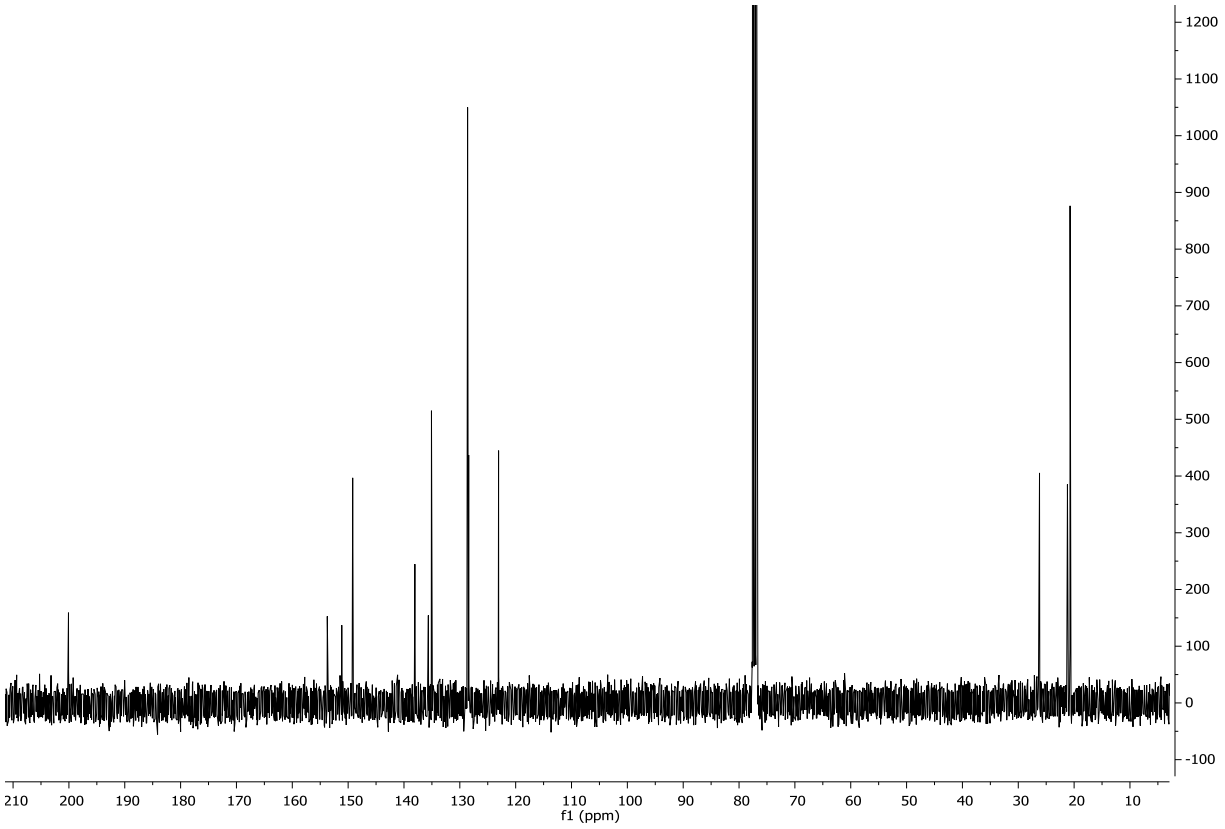

Figure S2. ^{13}C NMR spectrum of **7** in $CDCl_3$.

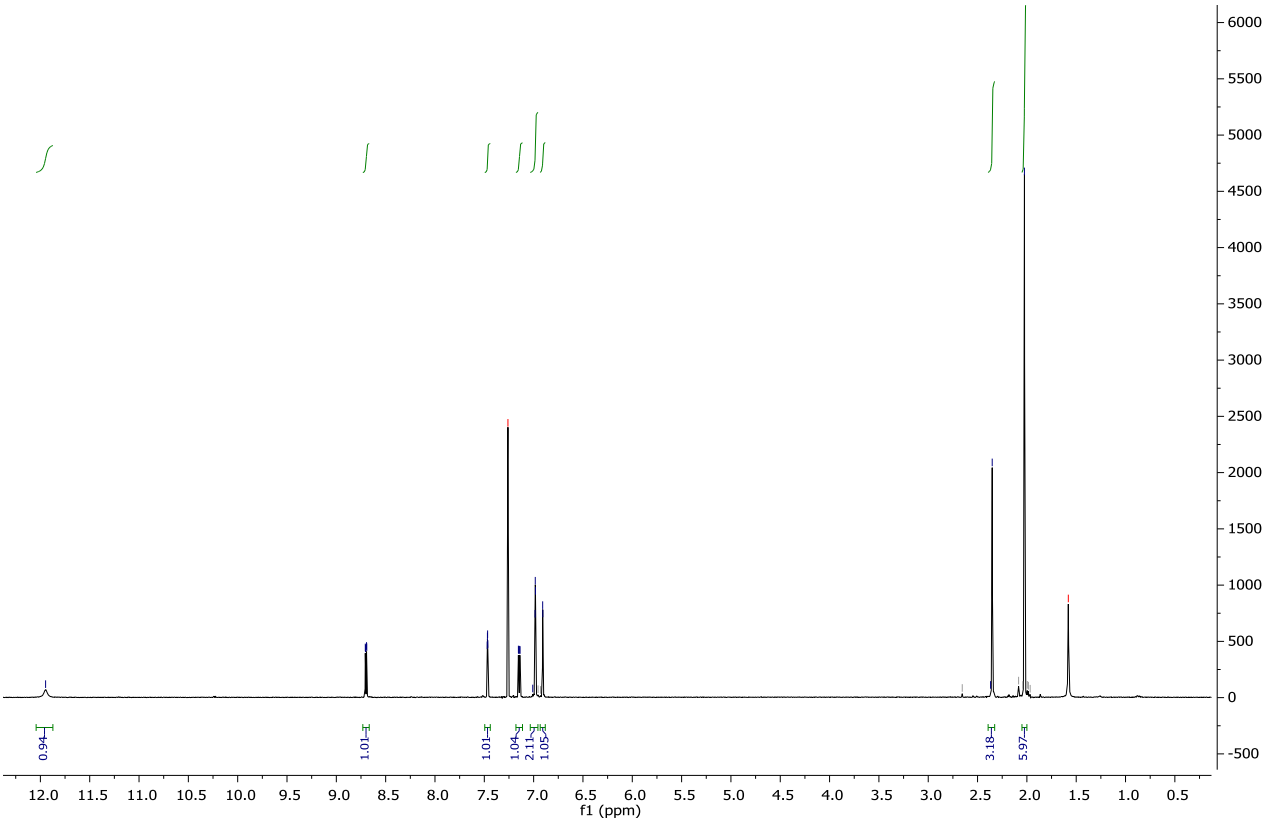

Figure S3. ^{1}H NMR spectrum of **9** in $CDCl_3$.

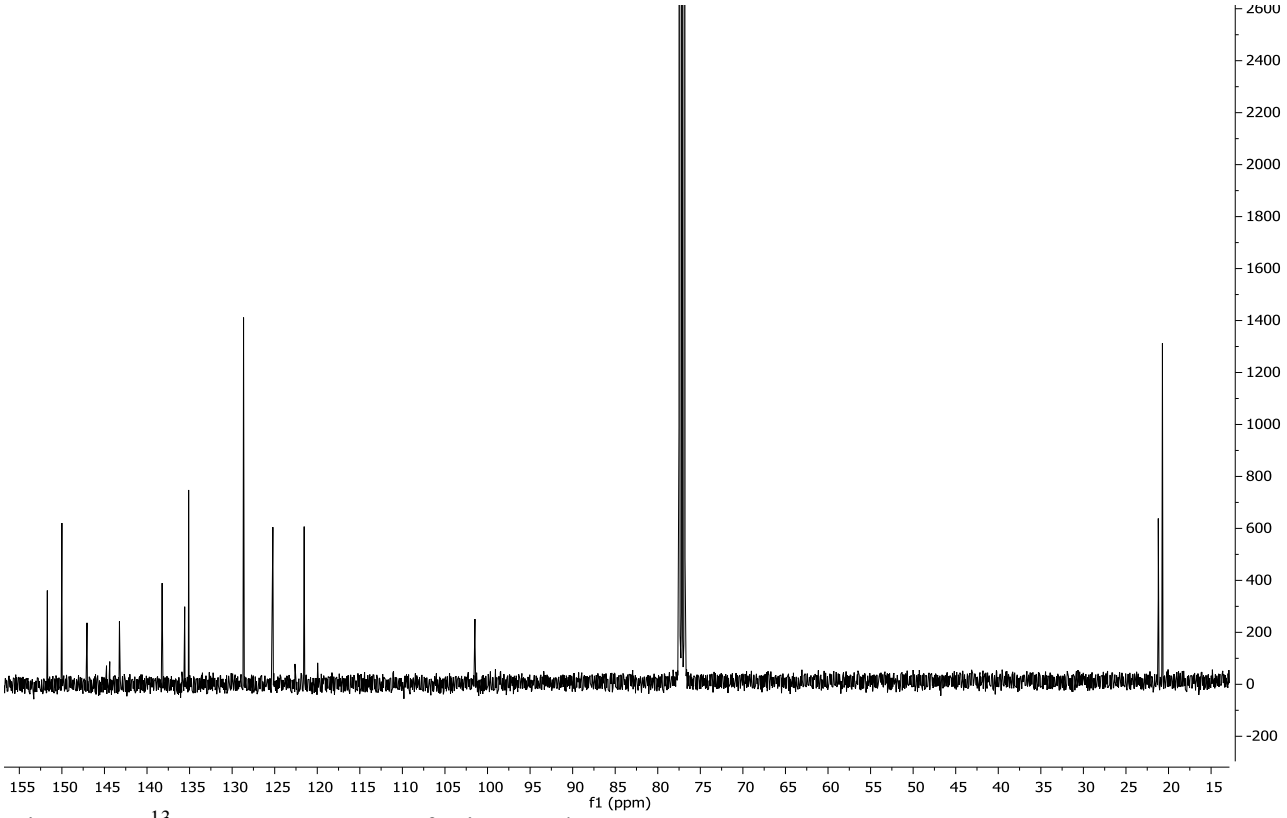

Figure S4. ^{13}C NMR spectrum of **9** in $CDCl_3$.

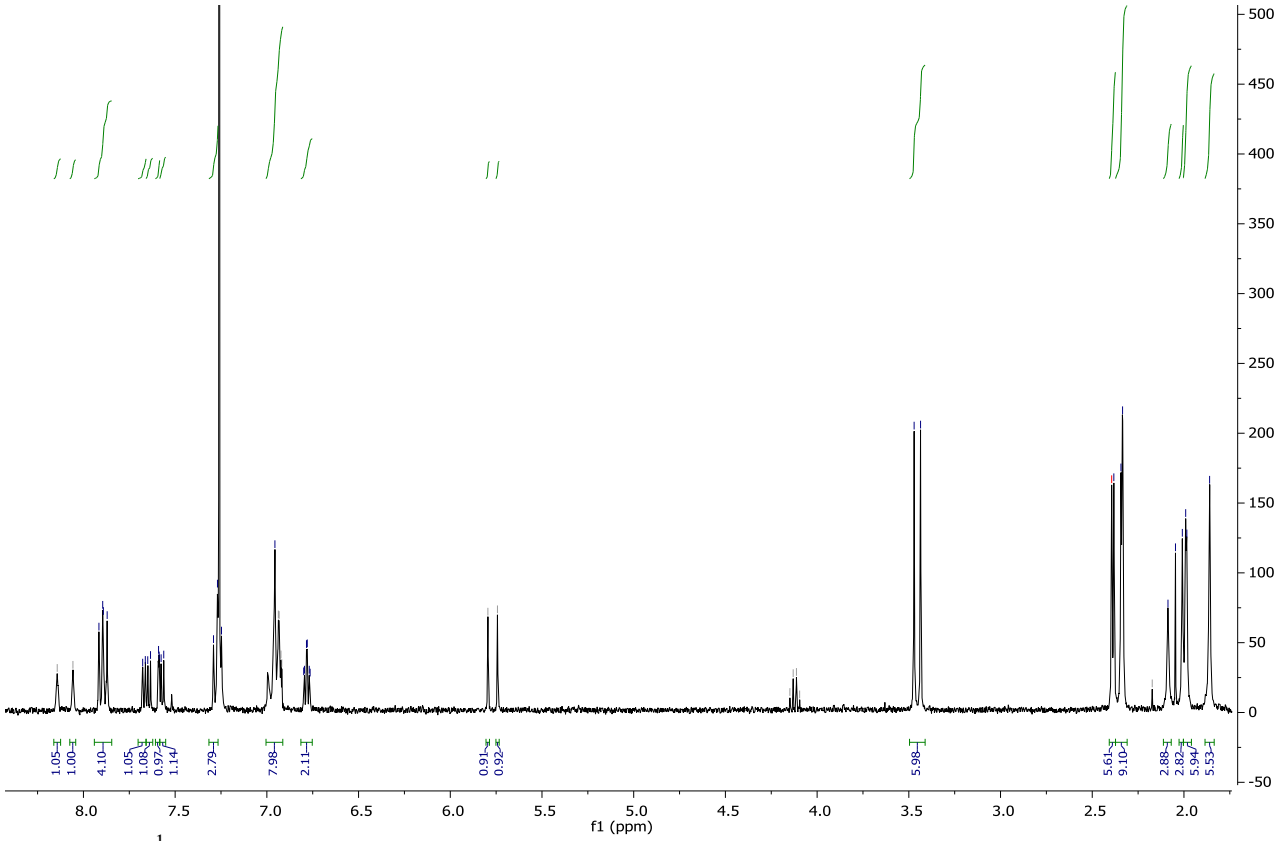

Figure S5. ^{1}H NMR spectrum of **12** in $CDCl_3$.

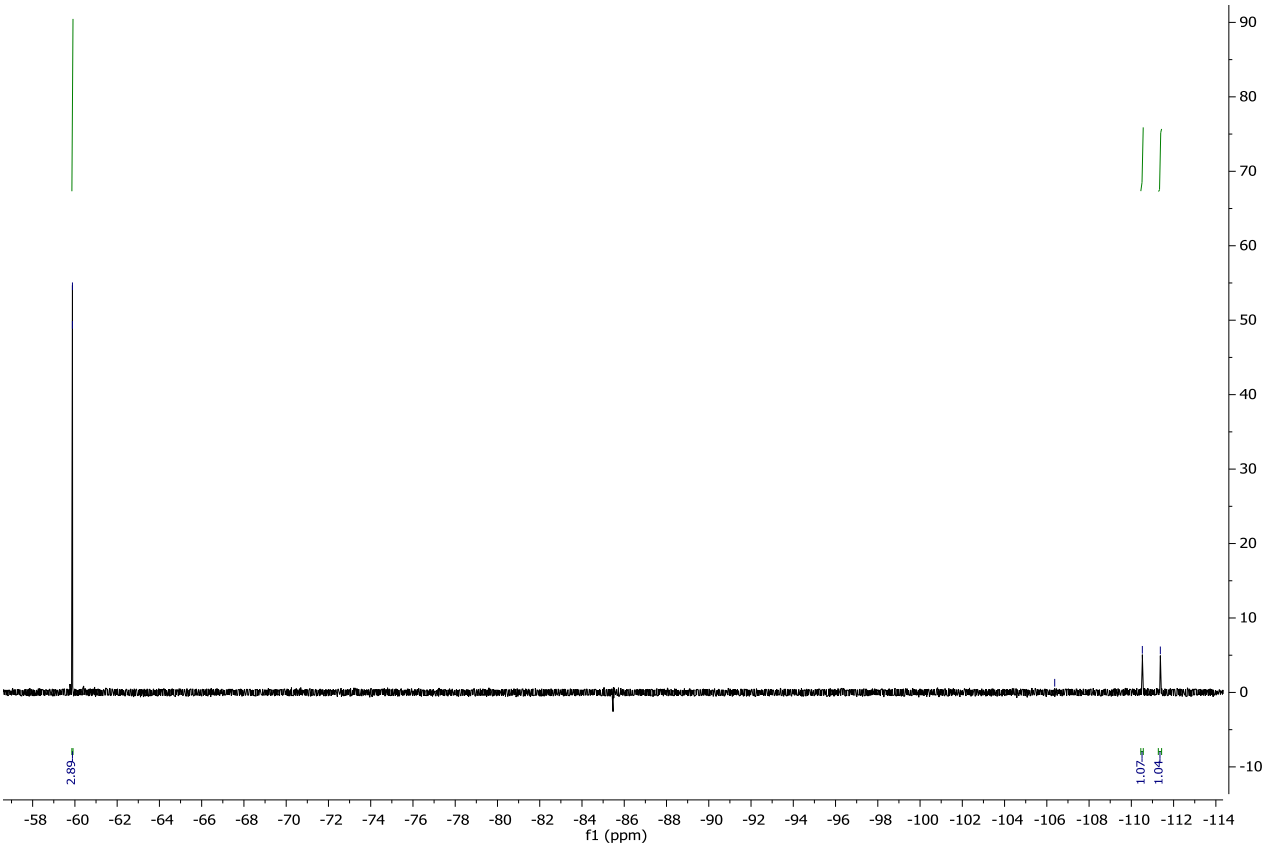

Figure S6. ^{19}F NMR spectrum of **12** in $CDCl_3$.

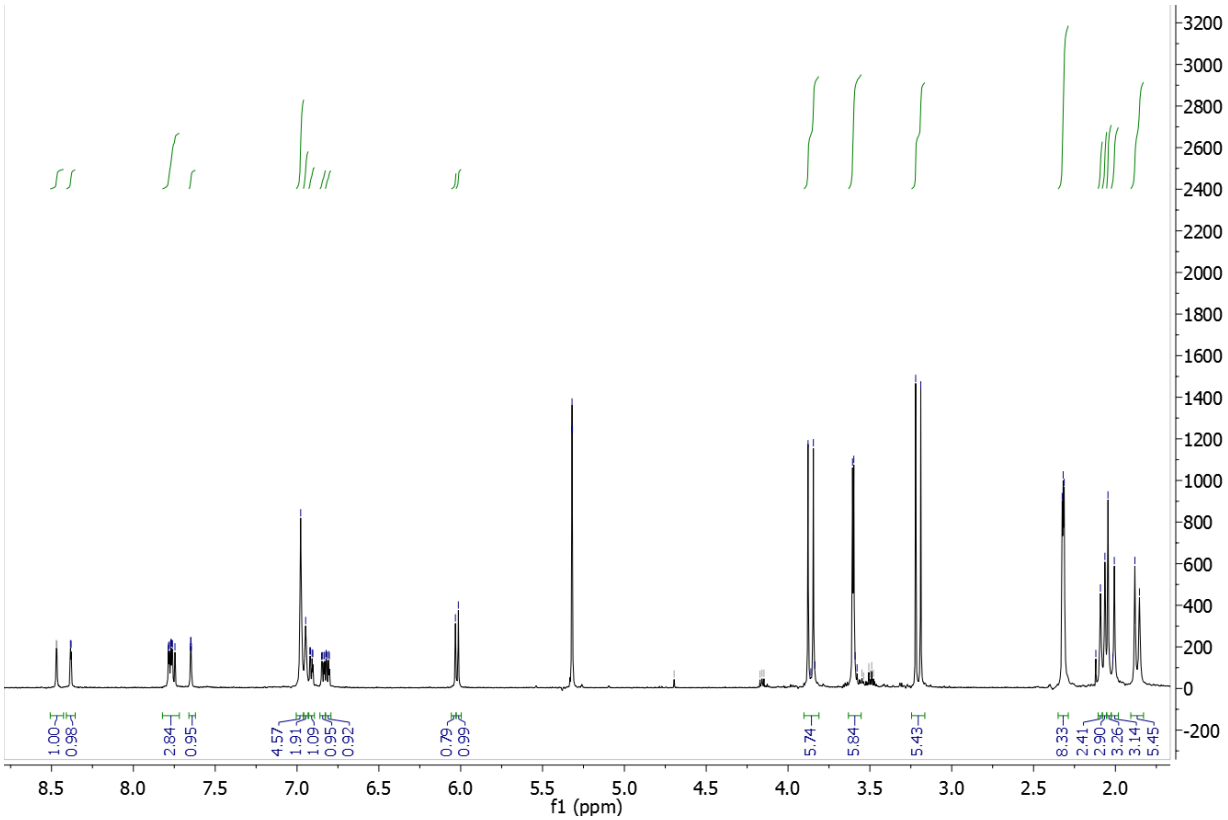

Figure S7. ^{1}H NMR spectrum of **13** in $CDCl_3$.

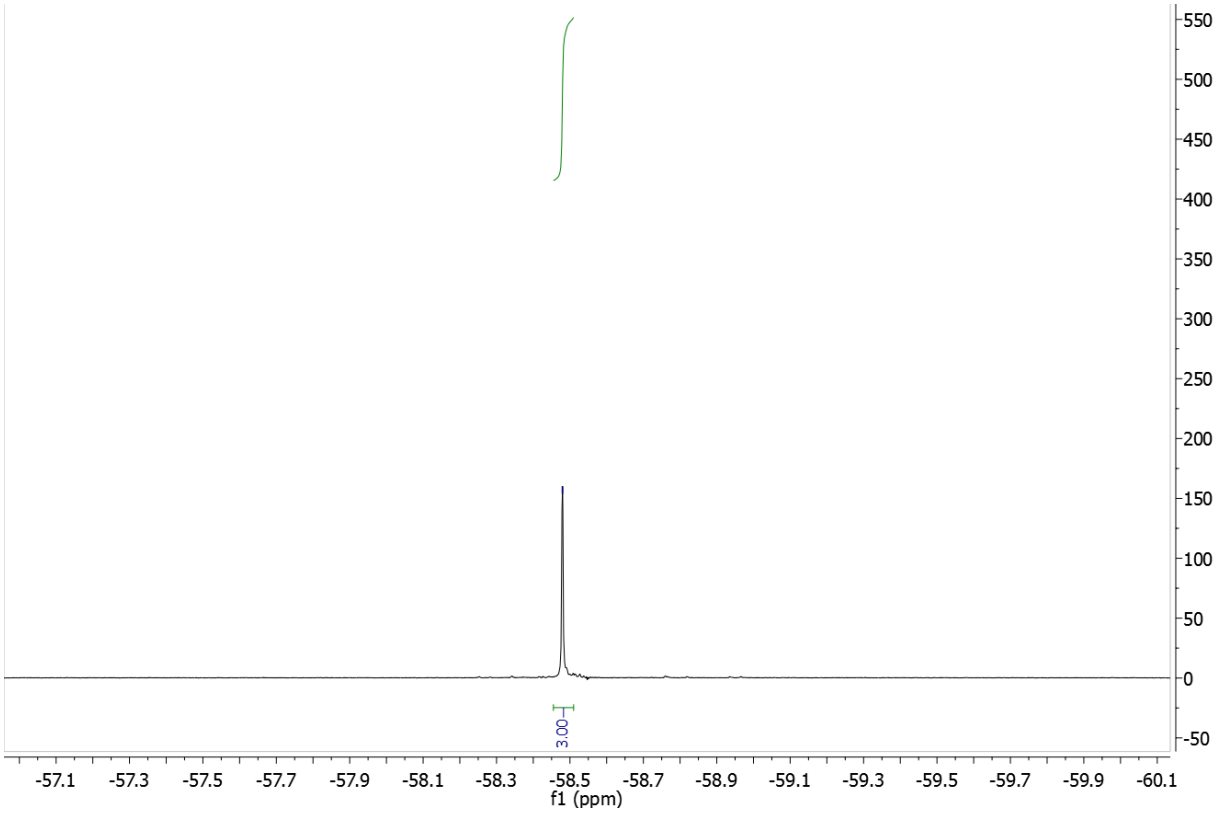

Figure S8. ^{19}F NMR spectrum of **13** in $CDCl_3$.

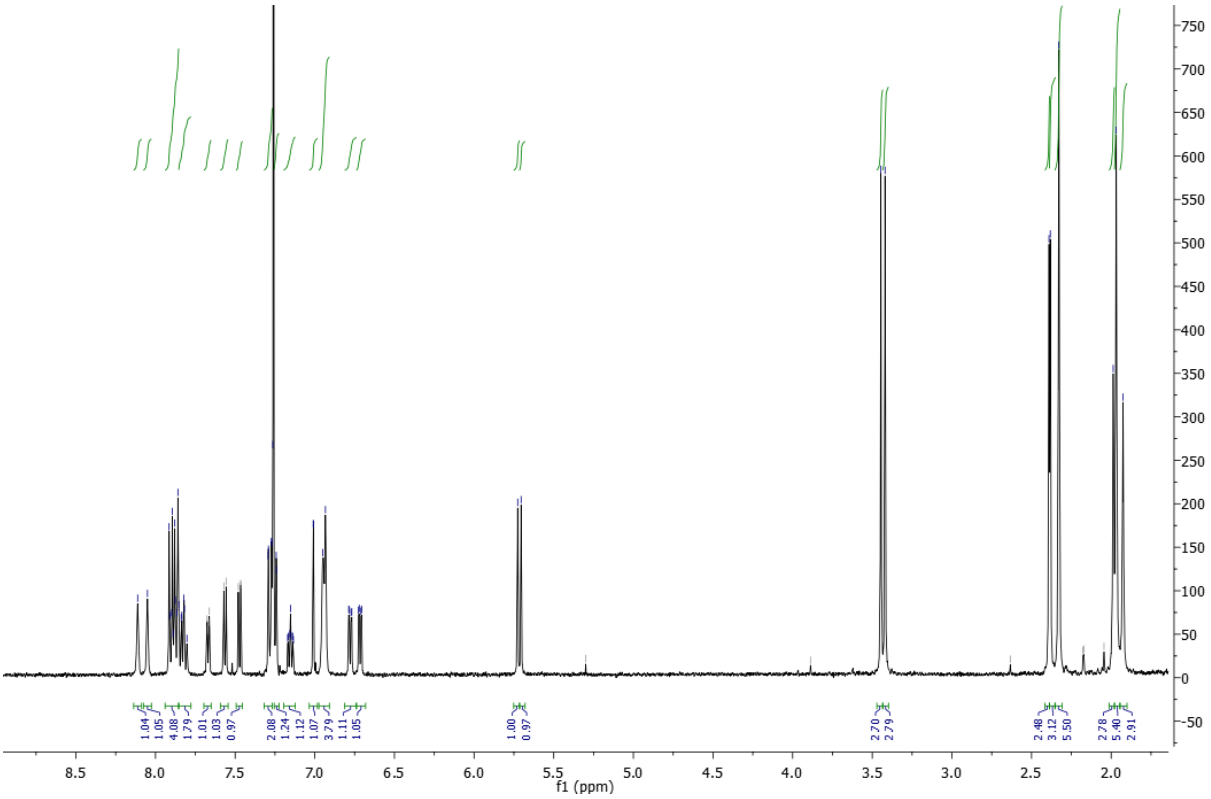

Figure S9. ^{1}H NMR spectrum of **14** in $CDCl_3$.

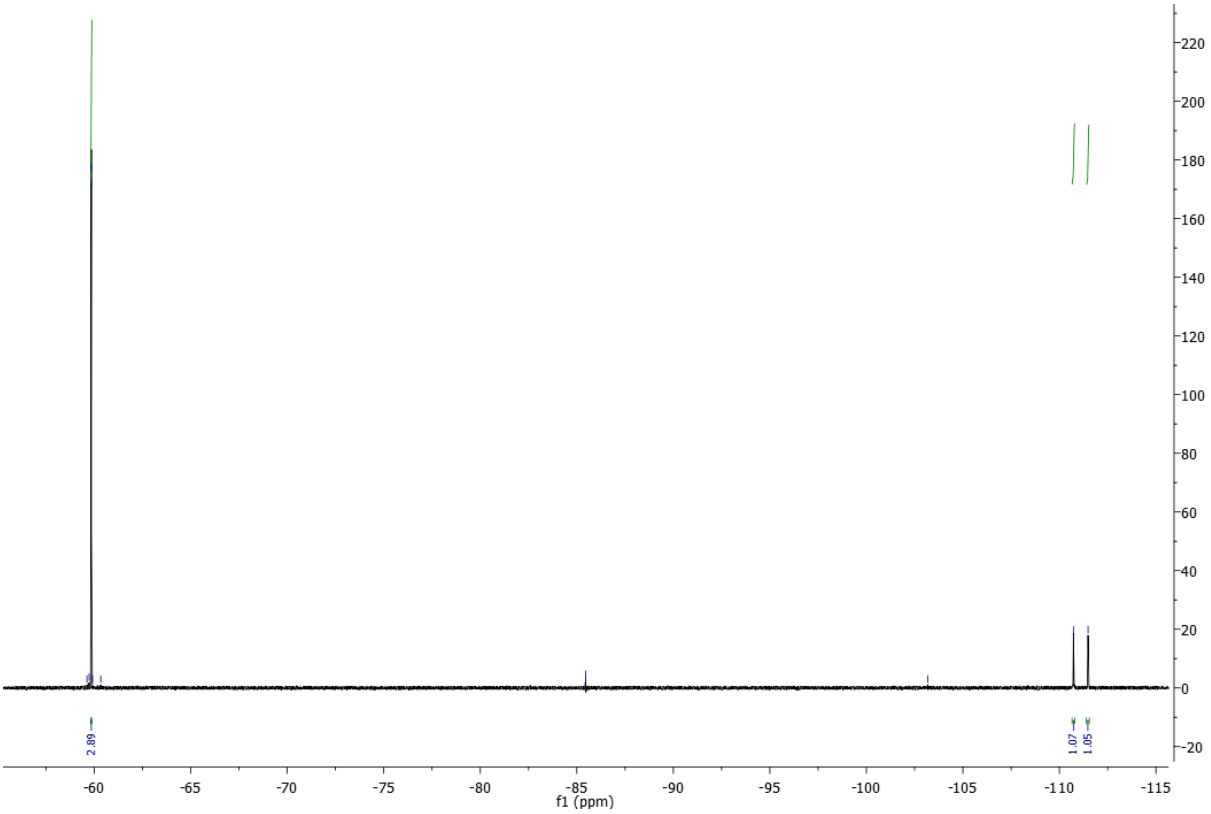

Figure S10. ^{19}F NMR spectrum of **14** in $CDCl_3$.

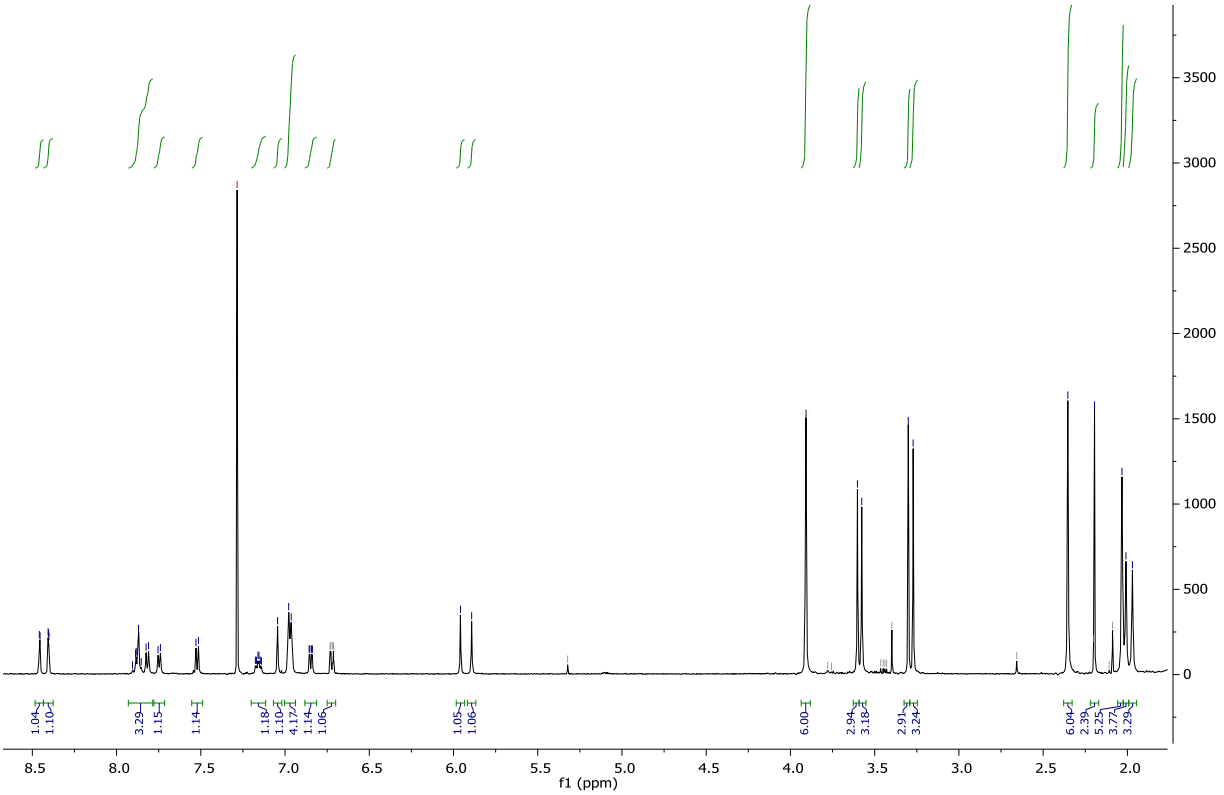

Figure S11. ^{1}H NMR spectrum of **15** in $CDCl_3$.

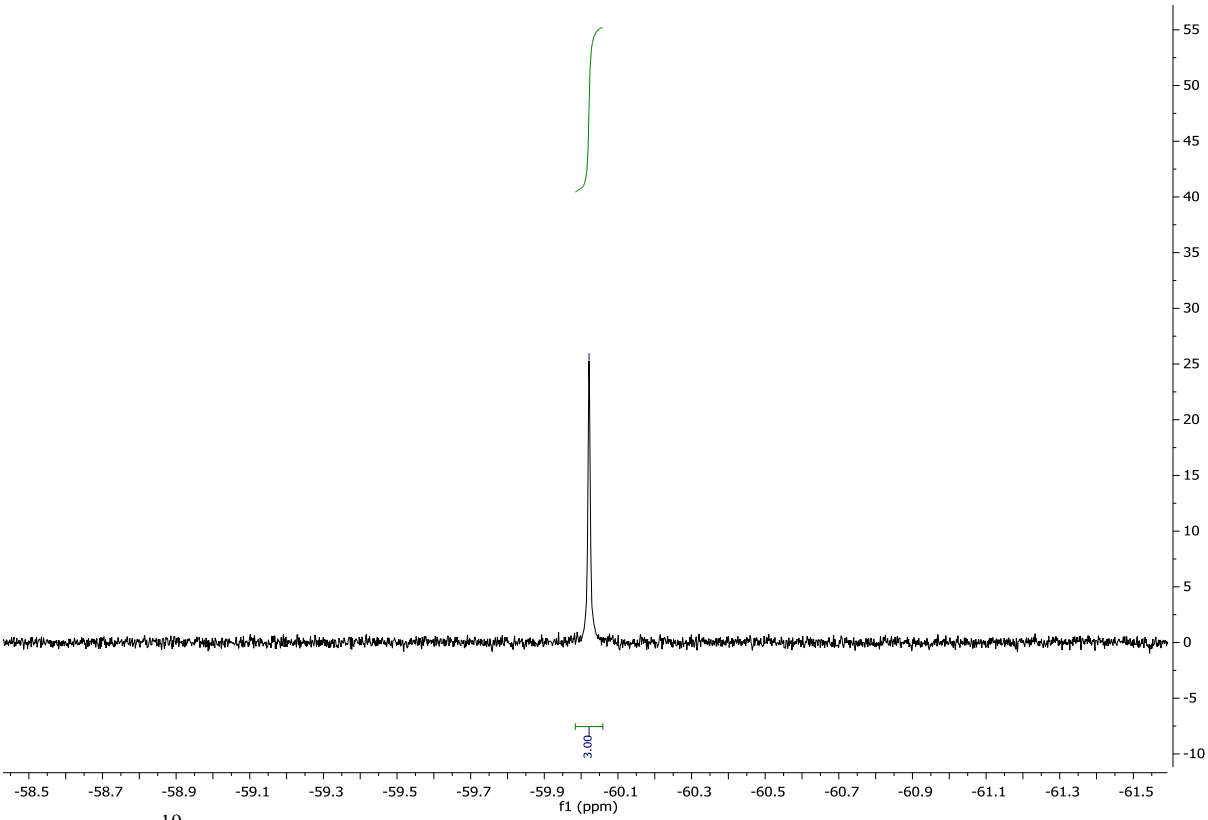

Figure S12. ^{19}F NMR spectrum of **15** in $CDCl_3$.

Table S1. MO energies and %MO contributions for important MOs in **12′**. Pz = pyrazylene, Py(pypz) = pyridylene in pypz ligand, Ph = phenylene, pyridylene in ppy ligand.

MO		eV	Pz	Py(pypz)	Ph	Ir	Py(ppy)
347	LUMO+3	-1.30	7	62	4	1	26
346	LUMO +2	-1.62	1	1	22	4	72
345	LUMO +1	-1.74	8	44	12	6	30
344	LUMO	-1.83	7	36	14	2	41
343	HOMO	-5.74	3	1	51	33	12
342	HOMO -1	-5.96	24	2	25	39	10
341	HOMO -2	-6.12	15	4	50	16	15
340	HOMO -3	-6.26	24	7	37	24	8

Table S2. MO energies and %MO contributions for important MOs in **13′**.

MO		eV	Pz	Py(pypz)	Ph	Ir	Py(ppy)
315	LUMO +3	-1.24	8	73	2	1	16
314	LUMO +2	-1.51	1	4	22	4	69
313	LUMO +1	-1.65	3	22	19	6	50
312	LUMO	-1.77	12	56	8	2	22
311	HOMO	-5.62	3	0	51	33	13
310	HOMO -1	-5.86	19	1	31	39	10
309	HOMO -2	-6.01	16	3	46	20	15
308	HOMO -3	-6.15	8	3	54	25	10

Table S3. MO energies and %MO contributions for important MOs in **14′**.

MO		eV	Pz	Py(pypz)	Ph	Ir	Py(ppy)
315	LUMO +3	-1.35	8	66	3	1	22
314	LUMO +2	-1.65	1	1	22	4	72
313	LUMO +1	-1.79	4	25	18	6	47
312	LUMO	-1.89	11	55	8	2	24
311	HOMO	-5.77	3	0	53	32	12
310	HOMO -1	-6.00	23	2	27	38	10
309	HOMO -2	-6.15	14	3	51	17	15
308	HOMO -3	-6.29	11	3	56	21	9

Table S4. MO energies and %MO contributions for important MOs in **15′**.

MO		eV	Pz	Py(pypz)	Ph	Ir	Py(ppy)
283	LUMO +3	-1.29	9	75	1	1	14
282	LUMO +2	-1.53	1	2	23	4	70
281	LUMO +1	-1.68	1	13	22	5	59
280	LUMO	-1.84	13	68	4	2	13
279	HOMO	-5.64	2	0	53	32	13
278	HOMO -1	-5.89	17	1	35	36	11
277	HOMO -2	-6.04	17	3	43	22	15
276	HOMO -3	-6.18	5	2	60	22	11

Cyclic voltammetry

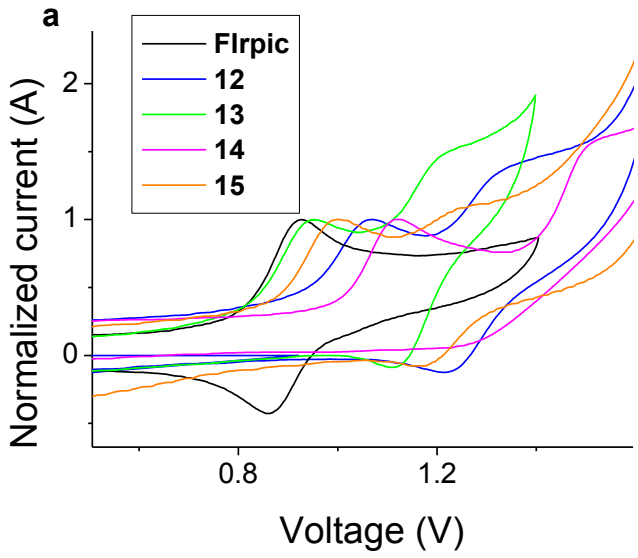

Figure S13. Cyclic voltammograms showing two oxidation waves for iridium complexes **12-15**.

Thermal properties

Table S5. Thermal stability data for all complexes using thermal gravimetric analysis (TGA) under a nitrogen atmosphere.

Complex	T_d (^oC)[a]
FIrpic (1)	370
1	387
2	367
12	351
13	306
14	300
15	316

[a] Defined as the 5% weight loss temperature.

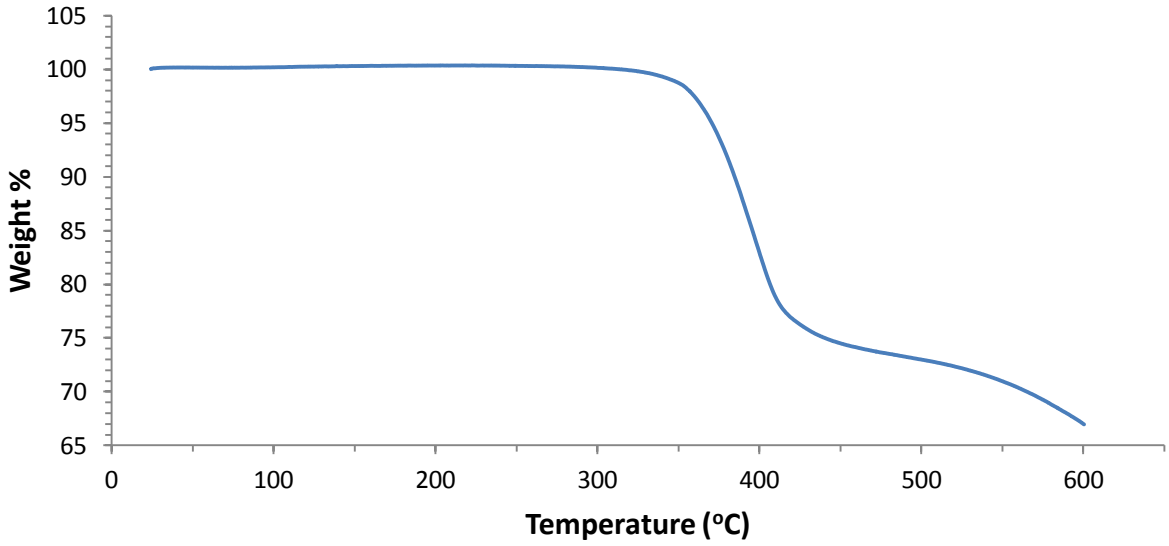

Figure S14. TGA curve for FIrpic.

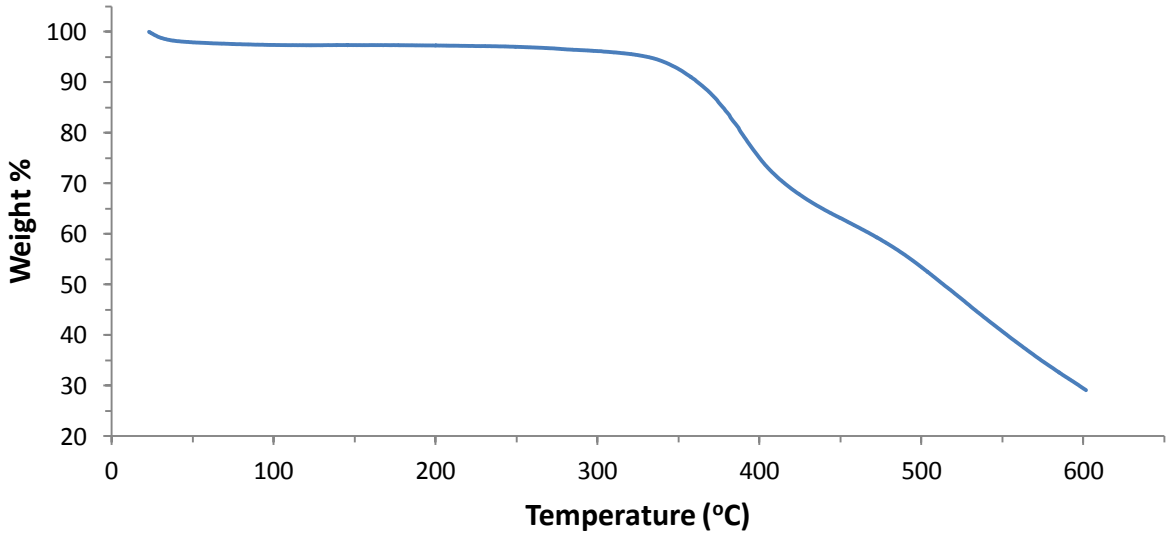

Figure S15. TGA curve for **12**. The T_d is determined after the initial solvent loss.

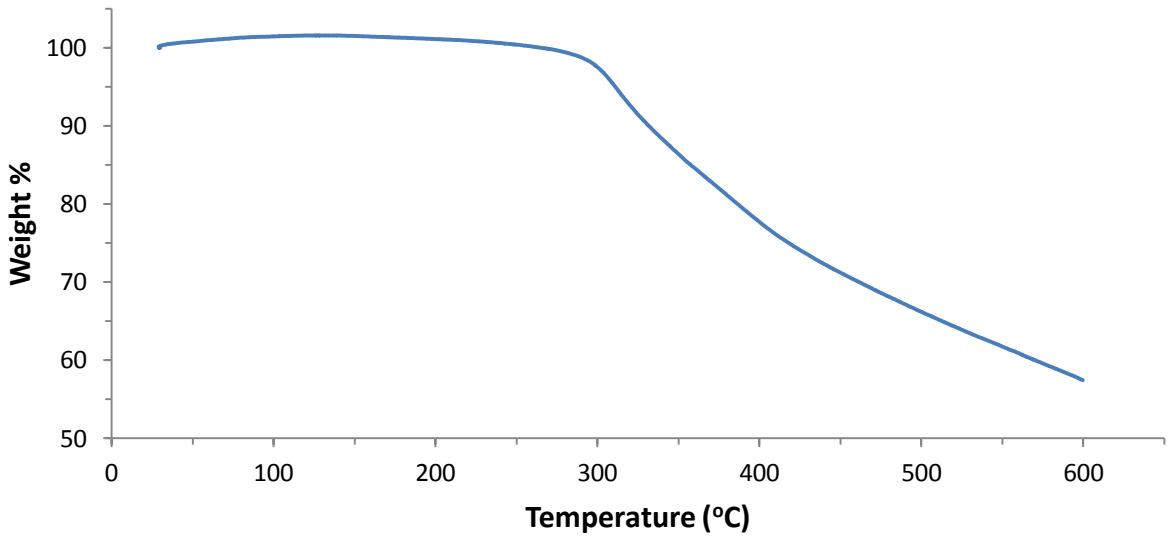

Figure S16. TGA curve for **13**.

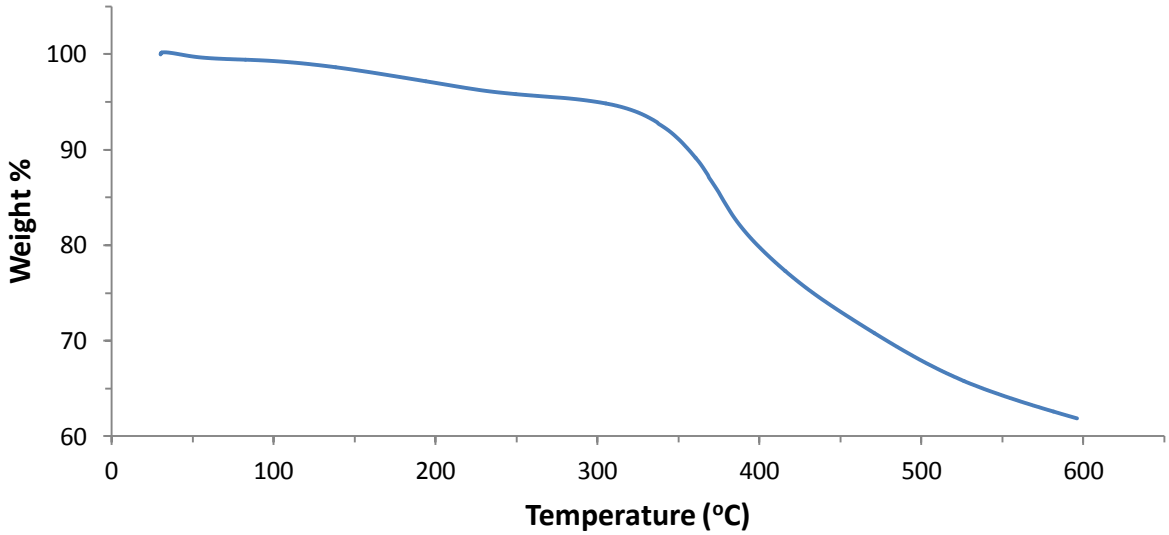

Figure S17. TGA curve for **14**.

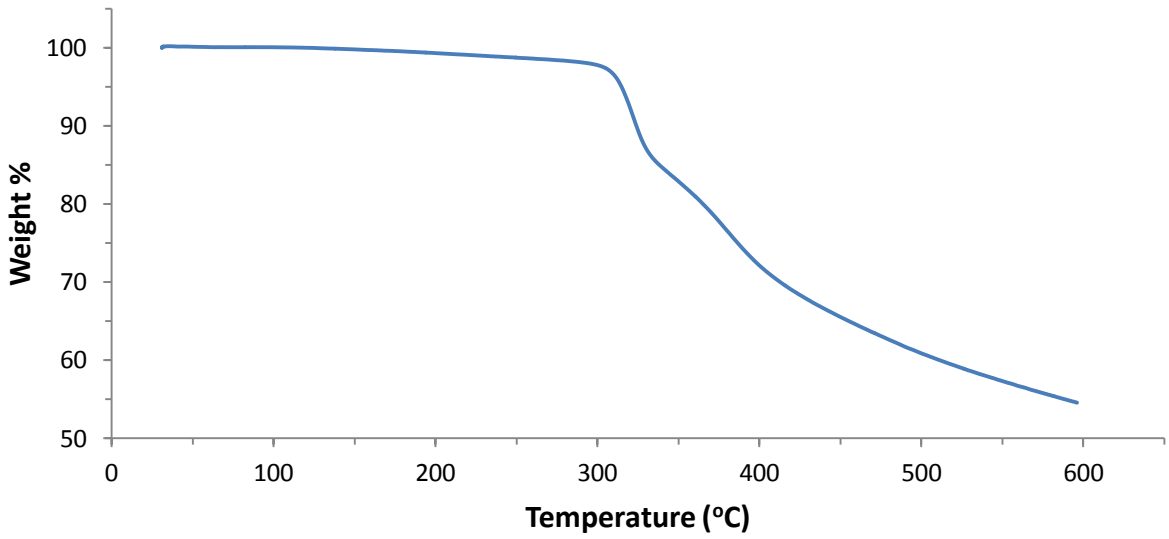

Figure S18. TGA curve for **15**.